Available online at www.sciencedirect.com
ScienceDirect
Journal of Catalysis 252 (2007) 258–270
JOURNAL OF CATALYSIS
www.elsevier.com/locate/jcat

Topological analysis of catalytic reaction networks: Methanol decomposition on Pt(111)

Saurabh A. Vilekar, Ilie Fishtik, Ravindra Datta *

Fuel Cell Center, Department of Chemical Engineering, Worcester Polytechnic Institute, Worcester, MA 01609, USA

Received 7 August 2007; accepted 22 September 2007

Available online 31 October 2007

Abstract

We describe our new reaction route (RR) graph approach as a powerful new tool for topological mechanistic and kinetic analysis of catalytic reaction networks, illustrated here with the help of methanol decomposition on Pt(111). In this approach a graph-theoretic network of molecular reaction steps is first constructed for the overall reaction (OR), on which each mechanistic step is represented by a directed branch interconnected at nodes, such that all conceivable reaction pathways can then be traced on it simply as walks or paths. Further, the network is consistent with the basic laws of flow graphs, so that it is suitable for a quantitative analysis. In fact, a direct analogy can be made to an equivalent wiring diagram, which allows tools of electric circuit analysis, namely, Kirchhoff's laws of current (rate) and potential (affinity), to be directly utilized for a rigorous flux analysis of the network. As a result, the dominant pathways as well as the rate-limiting steps (RLS) become transparent. This furthermore facilitates network pruning to retain only the essential steps and pathways. The RR graph approach when combined with *ab initio* kinetics, thus, provides a rigorous new framework for analyzing the mechanism and kinetics of catalytic reactions. It is, thus, found that methanol decomposition proceeds exclusively via the initial C–H dehydrogenation step rather than through O–H bond activation.

Keywords: Graph theory; Reaction network; Reaction pathways; Electrical analog; Kirchhoff's laws; Methanol decomposition

1. Introduction

With the advent of user-friendly quantum mechanics software, theoretical study of molecular catalytic reaction mechanisms has become rather commonplace as a very insightful tool [1–3]. Thus, until relatively recently, surface intermediates could only be guessed or identified via elaborate surface science experiments, whereas now, quantum chemistry calculations provide a detailed picture [4]. For instance, the optimized molecular structures of the reaction intermediates for methanol decomposition on Pt(111) are reported in detail in Refs. [5–9]. In fact, it is not even possible to experimentally detect all of these intermediates even with a broad array of sophisticated techniques including TPD, EELS, IRS, UPS, AES, and molecular beam [6]. First principle calculations can provide not only structural information but also thermochemical and energetic parameters for the surface reactions. In short, the density functional method (DFT) is an inimitable tool for determining the reaction intermediates and building a detailed molecular mechanism for catalytic reactions. The accuracy of predictions can be expected to only improve in the future.

However, this is only the starting point for developing a complete understanding of a catalytic system, including the most favorable reaction pathway and the key reaction steps. What is needed is an easy to use addendum to the quantum mechanical software that can utilize its first principles predictions to construct a comprehensive picture of the catalytic system, including elucidation of all parallel pathways and the dominant reaction routes and steps. While software tools such as CHEMKIN are available for this purpose, they are based on rather brute-force numerical methodologies. A more insightful graphic approach is called for that might be readily utilized by the catalytic scientist, without the necessity of being fully conversant with its theoretical underpinnings. We present such a consistent graph-theoretic approach and illustrate its simplicity

* Corresponding author.
E-mail address: rdatta@wpi.edu (R. Datta).

0021-9517/$ – see front matter
doi:10.1016/j.jcat.2007.09.020

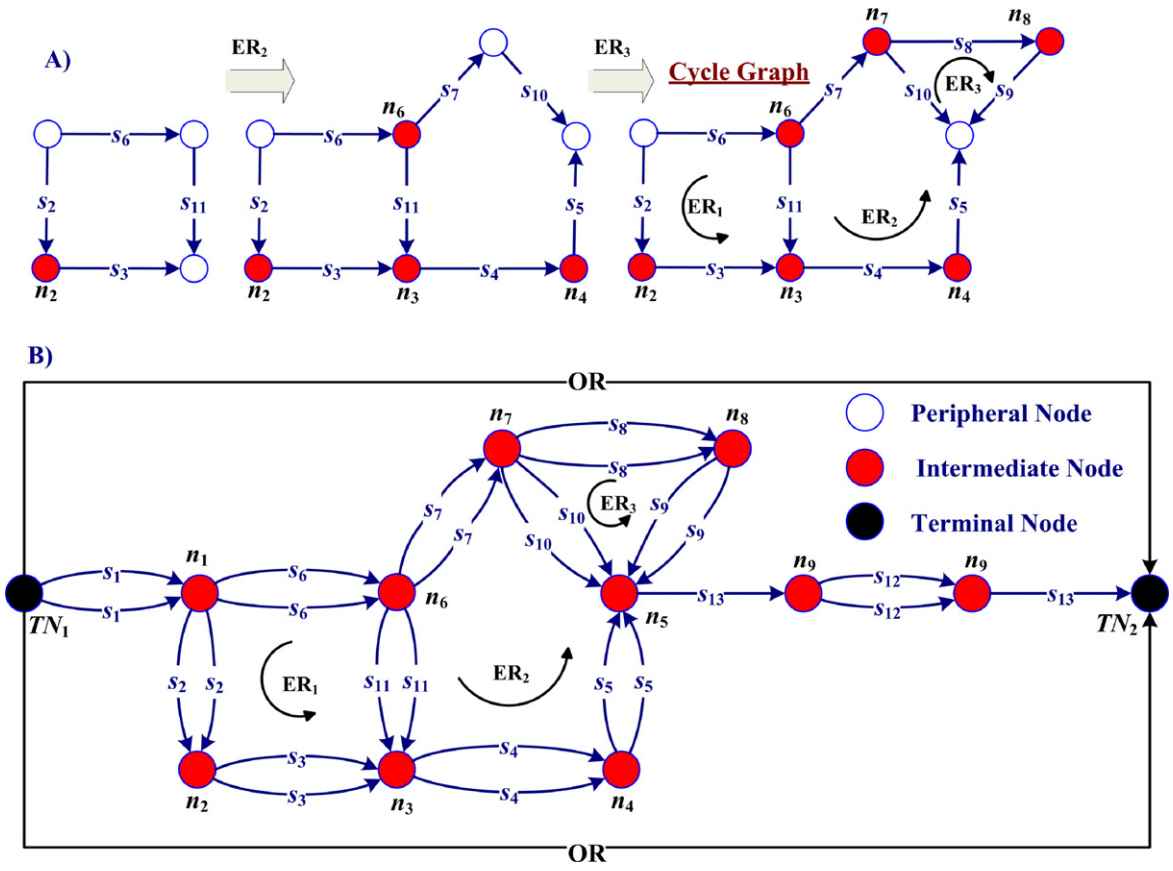

Fig. 1. Systematic construction of RR graph for methanol decomposition reaction.

and intuitive appeal with the help of methanol decomposition on Pt(111).

Graph-theoretical approaches to visualize reaction networks are, of course, not new [4,10,11]. Such mathematical depiction of network topology while useful is, however, not enough. Quantitative reaction networks involving flux of material must also conform to certain laws dealing with interdependence of flows in the interconnected networks, namely, mass balance at junctures, and consistency with thermodynamics. These, in fact, take the form of Kirchhoff's laws of current (charge balance) and potential (thermodynamic driving force) in electrical circuits [12], for instance. Thus, rules for graph-theoretic depiction of reaction networks need to be clearly enunciated and followed so that the resulting graphs are consistent with these basic requirements. Otherwise, the result is a little more than a pretty picture.

Unfortunately, practically all the existing reaction graph and theoretical approaches are inconsistent with these requirements, as is readily discerned, for instance, if one studies Fig. 1 of Broadbelt and Pfaendtner [4], which is inconsistent except for the case of linear mechanisms. Most catalytic mechanisms are non-linear although enzyme reactions are often linear. This is due to the unfortunate, but universal, practice of identifying nodes, or vertices with *individual* species, while branches, or edges, represent the reaction steps. This practice no doubt derives from the mechanisms depicted in chemistry texts, where species, often including structural details, are drawn at hubs interconnected by arrows depicting reactions. We describe here our new graph-theoretic approach that avoids this pitfall, overcoming the limitations of current methodologies and providing a self-consistent topological and mechanistic and kinetic analysis tool, based on the reaction route theory. The basic difference from the conventional approach is that the nodes, or hubs, do not necessarily represent an individual species, but rather simply represent the connectivity among elementary reaction steps in the network at a juncture. As a result, the RR graphs become quantitative that follow network laws. For instance, they can be directly converted into an equivalent electrical circuit, thus, allowing the well-developed and familiar methods of electric circuit theory, including Kirchhoff's laws, to be utilized in a direct and transparent fashion for network analysis. Thus, our new graph-theoretic approach, in conjunction with DFT calculations, forms a powerful combination for visualizing the myriad pathways, developing detailed network kinetics, and performing flux analysis and network pruning.

We present our approach without mathematical details [13–15] and using methanol decomposition on Pt(111) as an illustration, to show its utility in illuminating not only the reaction mechanism, but to also unequivocally judge the efficacy of the several competing parallel pathways and importance of reaction steps. DFT analysis of the nature and thermodynamics of the reaction intermediates in methanol decomposition was initially reported by Kua and Goddard [8] and by Ishikawa et al. [9], using a finite cluster model to represent the catalyst.

More recently, Cao et al. [7] have investigated the reaction intermediates and the mechanism for methanol decomposition on well-defined low Miller index platinum single crystal planes, Pt(111), Pt(110), and Pt(100), in an aqueous environment (in connection with direct methanol fuel cell), using a combination of chronoamperometry, fast scan cyclic voltammetry as well as an *ab initio*/DFT investigation using a three-layer periodic slab model. Their results support a dual path dehydrogenation mechanism, proceeding via both C–H and O–H bond activation of methanol.

For CH_3OH decomposition in the gas-phase (UHV) over Pt(111), Greeley and Mavrikakis [5,6] and Kandoi et al. [16] have also theoretically investigated the intermediates resulting from the homolytic C–H or O–H cleavage of methanol. In addition to thermodynamics, the Wisconsin group [5,6,16,17] has, also utilized the DFT method based on the extended-surface periodic-slab model, to determine the activation energy barriers for a 13-step mechanism comprising of both, the O–H and C–H bond scission pathways of methanol decomposition on Pt(111). This (Wisconsin) mechanism for methanol decomposition on Pt(111) comprising 13 elementary steps is adopted here, since it is the most comprehensive mechanism available providing many necessary details for our analysis (Table 1), to demonstrate our graph-theoretic reaction route (RR) network approach [13–15]. We show how this mechanism may be assembled into a RR graph, which may be converted into an equivalent reaction electrical circuit for further analysis, simplification, and pruning, using the standard tools of electric circuit analysis. The result is the emergence of an unambiguous picture of methanol decomposition on Pt(111), with a clear portrayal of all possible pathways, and irrefutable identification of the dominant pathways and rate limiting steps. This example, thus, clearly illustrates the utility of our approach in conjunction with DFT for unraveling catalyst reaction mechanism and kinetics.

2. Reaction route (RR) graphs: basic definitions

A reaction route (RR) or pathway is defined as a linear combination of elementary reactions steps s_ρ, such that a given number of species, either terminal (reactants and products) and/or intermediate, are eliminated [13–15] in the pathway. If all the intermediate species are eliminated, an overall reaction (OR) results, i.e., $\mathrm{OR} = \sum_\rho \sigma_\rho s_\rho$, and the corresponding pathway is referred to as full route, FR. For instance, from Table 1, $s_1 + s_6 + s_7 + s_{10} + s_{12} + 2s_{13} = \mathrm{OR}$, is a FR for methanol decomposition.

If all of the species, both intermediate and terminal, are eliminated in a given pathway, thus producing the so-called "zero" OR (i.e., the stoichiometric coefficients of all the species are equal to zero), the corresponding RR is called an empty route, ER, or simply a cycle, as more commonly known in Graph theory. For example, from Table 1, $s_2 + s_3 - s_6 - s_{11} = 0$, is an ER involved in the given mechanism. For complex mechanisms, the RRs, both FRs and ERs, can be numerous and are not unique. In fact, the RRs may be generated arbitrarily if no further stipulations are made. This is avoided by the concept of "directness," or minimality, following Milner [18] and Happel and Sellers [19]. Thus, a FR is a direct (or minimal) pathway if it is not possible to generate the OR if any elementary reaction is removed from the pathway, i.e., it contains no cycles. Such a direct FR contains no more than $q + 1$ steps, selected from among the given mechanism (Table 1), where q is the number of linearly independent intermediate species involved in the mechanism [13–15], typically one less than the number of intermediates due to site conservation. With this restriction on the path length, a finite set of FRs and ERs result, as shown in Table 4 for methanol decomposition. Their graphical generation is discussed later. The RR graphs constructed *must* be consistent with the basic requirement that all these FRs and ERs are evident on it as walks or paths.

Another basic difference of our RR graphs from the conventional reaction graphs is that the nodes in a RR graph simply represent reaction connectivity, in consistence with species mass balance and, in general, may represent a group of species and their properties rather than for an individual intermediate species. This freedom from arbitrarily identifying nodes with individual species completely alters the topology of the graph, which are now also consistent with flow network laws. It is further necessary to specify the rules that govern the connectivity of elementary reaction steps at the nodes of the RR network.

Table 1
The microkinetic model for methanol decomposition on Pt(111) [17]. The letter 'S' denotes a surface site. Activation energies and enthalpy changes in kJ/mol; the units of the pre-exponential factors are $\mathrm{atm}^{-1}\,\mathrm{s}^{-1}$ for adsorption/desorption reactions and s^{-1} for surface reactions

	$\vec{E}_\rho$	$\vec{A}_\rho$	Elementary reactions	$\overleftarrow{E}_\rho$	$\overleftarrow{A}_\rho$	ΔH^0_ρ
s_1	0	1.00E+06	$CH_3OH + S \rightleftarrows CH_3OH{\cdot}S$	31.845	8.64E+13	−31.845
s_2	60.795	1.04E+15	$CH_3OH{\cdot}S + S \rightleftarrows CH_3O{\cdot}S + H{\cdot}S$	18.335	1.12E+15	42.46
s_3	10.615	4.61E+14	$CH_3O{\cdot}S + 2S \rightleftarrows CH_2O{\cdot}S_2 + H{\cdot}S$	56.935	1.16E+15	−46.32
s_4	4.825	1.00E+13	$CH_2O{\cdot}S_2 \rightleftarrows CHO{\cdot}S + H{\cdot}S$	80.095	2.36E+12	−75.27
s_5	11.58	1.16E+14	$CHO{\cdot}S + S \rightleftarrows CO{\cdot}S + H{\cdot}S$	106.15	1.32E+15	−94.57
s_6	49.215	4.06E+15	$CH_3OH{\cdot}S + S \rightleftarrows CH_2OH{\cdot}S + H{\cdot}S$	76.235	1.12E+15	−27.02
s_7	41.495	2.99E+14	$CH_2OH{\cdot}S + S \rightleftarrows CHOH{\cdot}S + H{\cdot}S$	59.83	1.37E+15	−18.335
s_8	56.935	6.10E+13	$CHOH{\cdot}S + S \rightleftarrows COH{\cdot}S + H{\cdot}S$	116.765	2.72E+13	−59.83
s_9	77.2	7.87E+12	$COH{\cdot}S + S \rightleftarrows CO{\cdot}S + H{\cdot}S$	145.715	1.02E+14	−68.515
s_{10}	23.16	1.76E+13	$CHOH{\cdot}S + 2S \rightleftarrows CO{\cdot}S + 2H{\cdot}S$	151.505	1.01E+14	−128.345
s_{11}	51.145	1.95E+13	$CH_2OH{\cdot}S + 2S \rightleftarrows CH_2O{\cdot}S_2 + H{\cdot}S$	27.985	1.92E+14	23.16
s_{12}	133.888	1.00E+13	$CO{\cdot}S \rightleftarrows CO + S$	0	1.41E+05	133.888
s_{13}	88.2824	1.00E+13	$H{\cdot}S + H{\cdot}S \rightleftarrows H_2 + 2S$	13	6.33E+06	75.3

One of these is mentioned above, i.e., all FRs and ERs should be traceable as walks or paths. The other requirement is that the concept of directness or minimality is applicable to nodes as well, in the sense that for a "direct" node, it is not possible to satisfy the mass balance condition for a given set of species at that node, if a reaction is removed from the node. Further, there are two kinds of nodes on a RR graph, namely, intermediate nodes (INs), i.e., those that interconnect only elementary reaction steps, and terminal nodes (TNs), which also involve the overall reaction, i.e., OR. The intuitive generation of appropriate INs and TNs for methanol decomposition is discussed later. Mathematical details of the stoichiometric enumeration of direct RRs and direct nodes for a given mechanism may be found in our previous publications [13–15], but this procedure is not followed here for simplicity.

The RR graph drawn in conformity to the above rules is also "direct" or minimal. Furthermore, it is consistent with conservation of mass at the nodes as well as with the thermodynamic constraints, i.e., path independence of thermodynamic potentials. Thus, Gibbs free energy (or enthalpy) of steps must add up to that of the OR in a FR, and it must be zero for an ER. Clearly, any quantitative network involving flow of an entity (e.g., a piping system) must be consistent with these two basic laws of networks.

In this regard, it is useful to draw an analogy of RR networks to electrical networks, which are familiar to most of us and the analysis of which is developed to a high degree of sophistication [12]. The applicable network laws of electrical circuits are, of course, the Kirchhoff's laws of current (flow) and potential (thermodynamics). Therefore, an analogy between RR networks and electrical networks is illuminating, and is described here.

Since it follows flow network laws, RR graph can be directly converted into an equivalent electric circuit, or wiring diagram, thus greatly facilitating its analysis by allowing use of the vast array of techniques available for electric circuit analysis. Further, each branch in the RR network may be replaced by its impedance, or "resistance" R_ρ for the steady-state case, while the branch representing the OR is replaced by a "voltage" source, A_{OR}, i.e., the affinity (or $-\Delta G_{\mathrm{OR}}$, the Gibbs free energy change) of the OR. The branch "voltage" is $A_\rho(=-\Delta G_\rho)$ i.e., the reaction step affinity. This allows utilization of the well-established methodologies of circuit analysis [12], including Kirchhoff's laws and nodal and loop analyses, in RR network analyses.

Since the nodes simply represent the connectivity, and thus have a zero capacity, the net rates r_ρ of reactions or branches (akin to branch current, I_ρ) incident at the jth node (intermediate and terminal) sum to zero

$$\sum_{\rho=1}^{p} m_{j\rho} r_\rho = 0 \quad (j = 1, 2, \ldots, n), \tag{1}$$

where $m_{j\rho} = +1$ if a branch is incident from a node; while $m_{j\rho} = -1$ if a branch is incident to it. In fact $m_{j\rho}$ are elements of the incidence matrix of the RR graph [13]. Equation (1) is the equivalent of Kirchhoff's Current Law (KCL) for electrical circuits, and results from a linear combination of the quasi-steady state (QSS) condition for individual species [14]. Furthermore, being a state function, the sum of reaction affinities $(A_\rho = -\Delta G_\rho)$ [14], akin to branch voltages V_ρ, around the ER is

$$\mathrm{ER}_w\colon \quad \sum_{\rho=1}^{p} \sigma_{w\rho} A_\rho = 0 \quad \text{or}$$

$$\prod_{\mathrm{ER}_w} K_\rho^{\sigma_{w\rho}} = 1 \quad (w = 1, 2, \ldots, P), \tag{2}$$

which is the equivalent of Kirchhoff's Potential Law (KPL), and ensures thermodynamic consistence of rate constants [13–15], calculated from *ab initio* [20] or semi theoretical methods [21]. In fact, this reduces the number of rate constants that must be determined. A similar relation exists for the FRs between branch and OR affinity and, hence, equilibrium constants.

Finally, to complete the electrical analogy, the reaction kinetics may also be written *rigorously* in the form of Ohm's law [13], although, of course, the kinetics do not conform to a linear constitutive relation. This step is not necessary, of course, since Kirchhoff's Laws apply for nonlinear elements, e.g. diodes, as well, but is intuitively appealing. It results from the following definitions for the net rate of a reaction step s_ρ and its affinity A_ρ [13]

$$r_\rho = \vec{r}_\rho - \overleftarrow{r}_\rho; \quad \mathcal{A}_\rho = \frac{A_\rho}{RT} = \ln \frac{\vec{r}_\rho}{\overleftarrow{r}_\rho} \quad (\rho = 1, 2, \ldots, p). \tag{3}$$

The reaction resistance R_ρ, i.e., the inverse of reaction conductance, is defined [13] as the mean value of the $1/r_\rho$ between its limiting values, namely, $\vec{r}_\rho$ and $\overleftarrow{r}_\rho$:

$$R_\rho = \frac{1}{\vec{r}_\rho - \overleftarrow{r}_\rho} \int_{\overleftarrow{r}_\rho}^{\vec{r}_\rho} \frac{1}{r_\rho}\, dr_\rho$$

$$= \frac{\ln(\vec{r}_\rho/\overleftarrow{r}_\rho)}{\vec{r}_\rho - \overleftarrow{r}_\rho} = \frac{\mathcal{A}_\rho}{r_\rho} \quad (\rho = 1, 2, \ldots, p), \tag{4}$$

which, thus provides a linear relation between $\mathcal{A}_\rho$ and r_ρ, in the form of Ohm's law, albeit R_ρ changes with reaction conditions, i.e., composition, and especially temperature. With this, the analogy between RR networks and electrical circuits is complete, thus putting this oft-used intuitive analogy in texts [22] on a rigorous footing.

3. Case study: methanol decomposition on Pt(111)

The $p = 13$ elementary reaction steps comprising the mechanism of methanol decomposition on Pt(111) developed by, Greeley and Mavrikakis [6] and Gokhale et al. [17], is adopted here for illustrating our RR graph approach, and is summarized in Table 1. The mechanism consists of two initial dehydrogenation pathways, one proceeding via O–H bond scission (step s_2) and the other proceeding via C–H bond scission (step s_6). Steps s_1, s_{12} and s_{13} are the adsorption–desorption steps for methanol, carbon monoxide and hydrogen respectively, while the rest are

all surface reaction steps. All reactions are considered to be reversible. The extent of reversibility of a step, of course, varies and is indicated by its affinity, A_ρ.

Gokhale et al. [17] have also provided the thermodynamic properties of the surface intermediate species, $I_k{\cdot}S$, based on the DFT prediction of the total electronic energy (TE) of the system and the vibrational spectra of the species. Thus, the standard enthalpy of formation of a surface species was calculated by them via

$$H^0_{I_k\cdot S} = H^0_{I_{k(g)}} + BE_{I_k\cdot S} + \Delta(ZPE_{I_k}), \tag{5}$$

where $H^0_{I_k(g)}$ is the standard enthalpy of formation in the gas phase, $BE_{I_k\cdot S}$ is the binding energy, and $\Delta(ZPE_{I_k})$ is the zero point energy correction to binding energy of the intermediate species I_k, all of which are provided by Gokhale et al. [17]. The thermodynamic properties of the surface reaction steps were then calculated by them based on the species thermodynamic properties. Thus, for the surface reaction s_ρ, defined as

$$\sum_{k=1}^{l} \alpha_{\rho k} I_k{\cdot}S + \sum_{i=1}^{n} \beta_{\rho i} T_i = 0. \tag{6}$$

The enthalpy change and the entropy change are

$$\Delta H^0_\rho = \sum_{k=1}^{l} \alpha_{\rho k}\left(H^0_{I_k\cdot S}\right) + \sum_{i=1}^{n} \beta_{\rho i}\left(H^0_{T_i(g)}\right) \quad \text{and}$$

$$\Delta S^0_\rho = \sum_{k=1}^{l} \alpha_{\rho k}\left(S^0_{I_k\cdot S}\right) + \sum_{i=1}^{n} \beta_{\rho i}\left(S^0_{T_i(g)}\right), \tag{7}$$

where $\alpha_{\rho k}$ is the stoichiometric coefficient of surface intermediate $I_k{\cdot}S$ ($k = 1, 2, \ldots, l$) and $\beta_{\rho i}$ of the terminal species T_i ($i = 1, 2, \ldots, n$), in the reaction step s_ρ.

The standard entropy of formation of a surface species, $I_k{\cdot}S$ is based on the assumption that adsorption causes a total loss of translational entropy [23], i.e.,

$$S^0_{I_k\cdot S} = S^0_{I_k(g)} - S_{trans,I_{k(g)}}, \tag{8}$$

where $S^0_{I_k(g)}$ is the standard entropy of formation and $S_{trans,I_{k(g)}}$ is the translational entropy of the species I_k in the gas phase

$$S_{trans,I_{k(g)}} = R\left[\frac{5}{2} + \ln\left(\frac{(2\pi m k_B T)^{3/2}\upsilon_{I_k(g)}}{h^3}\right)\right], \tag{9}$$

where $\upsilon_{I_k(g)}$ is the molar volume of gas-phase I_k. The entropy values for species in the gas phase, $S^0_{I_k(g)}$ were taken from standard handbooks [24–26]. The entropies of formation of CHOH and COH in the gas phase were, however, determined by us using Gaussian 03 [27] at the B3LYP/LANL2DZ level of theory with harmonic oscillator approximation, at reference temperature of 298 K and 1 bar, due to lack of reported values in the literature. The vibrational frequencies, thus, predicted were similar to those reported by Gokhale et al. [17].

The forward and reverse rate constants in Table 1 are written in the Arrhenius form

$$\vec{k}_\rho = \vec{A}_\rho \exp\left(-\frac{\vec{E}_\rho}{RT}\right); \quad \overleftarrow{k}_\rho = \overleftarrow{A}_\rho \exp\left(-\frac{\overleftarrow{E}_\rho}{RT}\right) \quad \text{and}$$

$$\vec{E}_\rho - \overleftarrow{E}_\rho = \Delta H^0_\rho, \tag{10}$$

where A_ρ are the pre-exponential factors. The activation energies for steps s_2 through s_{11} were taken from Ref. [17] and are based on DFT calculations, while those for the adsorption and desorption steps (s_1, s_{12}, s_{13}), not provided in Ref. [17] were calculated by us using the UBI-QEP method [21], which is based solely on the heats of chemisorption and bond dissociation energies of the species involved, already available.

The pre-exponential factors in the exothermic direction were taken from Ref. [17], while the ones in the reverse direction were calculated by us from the standard reaction entropies as estimated above and the following relation [23], to ensure thermodynamic consistency with the known thermodynamics of the overall reaction:

$$\overleftarrow{A}_\rho = \vec{A}_\rho \cdot \exp\left(-\Delta S^0_\rho / R\right). \tag{11}$$

The pre-exponential factors listed in Table 1 were not subsequently varied from these initial estimates. It must be noted, that there some differences between the Wisconsin model and ours, especially, the methodology for calculation of the pre-exponential factors in the reverse direction. Moreover, for the sake of simplicity, we have not utilized binding energy of CO as a function of surface coverage.

4. Enumeration of RRs and nodes

The first step in our RR graph approach is the enumeration of the reaction routes, or pathways [19]. Then, the RR graph is drawn on which all the RRs can be traced as walks or paths. According to the stoichiometric RR formalism, the species comprising the mechanism are divided into terminal, i.e., reactants (CH_3OH) and products (CO and H_2), and, surface intermediates (S, $CH_3OH{\cdot}S$, $CH_2OH{\cdot}S$, $CHOH{\cdot}S$, $COH{\cdot}S$, $CH_3O{\cdot}S$, $CH_2O{\cdot}S_2$, $CHO{\cdot}S$, $CO{\cdot}S$ and $H{\cdot}S$) where S stands for a free active site on the catalyst surface. Due to the site conservation, however, only $q = 9$ out of $l = 10$ intermediates are linearly independent.

According to Horiuti–Temkin theorem, only $\mu = p - q = 13 - 9 = 4$ RRs are linearly independent from the *complete* set of enumerated FRs and ERs for this system. Any appropriate set may be chosen. Moreover, the number of linearly independent ERs is given by $p - (q + 1) = 13 - 9 - 1 = 3$ for the reaction mechanism considered [13–15]. Thus, a set of 4 linearly independent RRs may be readily determined by finding 3 independent ERs and one FR for the mechanism. These, in fact, can be determined simply from an inspection of the mechanism, thus avoiding the step of systematic stoichiometric enumeration as described in our earlier publications [13–15]. In fact, as shown here, all these FRs and ERs can be determined topologically as walks, once the RR graph is constructed.

A direct FR for this system, as defined earlier, involves no more than $q + 1 = 9 + 1 = 10$ elementary steps. Many may include fewer steps. A simple inspection of the reaction mechanism (Table 1) shows that $s_1 + s_2 + s_3 + s_4 + s_5 + s_{12} + 2s_{13} =$

Table 2
QSS conditions for surface intermediates and terminal species involved in methanol decomposition

Intermediate species	
$CH_3OH{\cdot}S$ (Q_1)	$r_1 - r_2 - r_6 = 0$
$CH_3O{\cdot}S$ (Q_2)	$r_2 - r_3 = 0$
$CH_2O{\cdot}S_2$ (Q_3)	$r_3 - r_4 + r_{11} = 0$
$CHO{\cdot}S$ (Q_4)	$r_4 - r_5 = 0$
$CO{\cdot}S$ (Q_5)	$r_5 + r_9 + r_{10} - r_{12} = 0$
$H{\cdot}S$ (Q_6)	$r_2 + r_3 + r_4 + r_5 + r_6 + r_7 + r_8 + r_9 + 2r_{10} + r_{11} - 2r_{13} = 0$
$CH_2OH{\cdot}S$ (Q_7)	$r_6 - r_7 - r_{11} = 0$
$CHOH{\cdot}S$ (Q_8)	$r_7 - r_8 - r_{10} = 0$
$COH{\cdot}S$ (Q_9)	$r_8 - r_9 = 0$
Terminal species	
CH_3OH	$r_1 = r_{OR}$
CO	$r_{12} = r_{OR}$
H_2	$r_{13} = 2r_{OR}$

Table 3
List of intermediate and terminal nodes for the 13-step methanol decomposition reaction mechanism

Intermediate nodes	
$IN_1 = s_1 - s_2 - s_6$	$IN_{17} = 2s_4 + 2s_8 + 2s_{10} - s_{13}$
$IN_2 = s_2 - s_3$	$IN_{18} = 2s_4 + 2s_7 - s_{13}$
$IN_3 = s_3 - s_4 + s_{11}$	$IN_{19} = 2s_4 + 2s_6 - 2s_{11} - s_{13}$
$IN_4 = s_4 - s_5$	$IN_{20} = 2s_3 + 2s_9 + 2s_{10} + 2s_{11} - s_{13}$
$IN_5 = 2s_5 + 2s_9 + 2s_{10} - s_{13}$	$IN_{21} = 2s_3 + 2s_8 + 2s_{10} + 2s_{11} - s_{13}$
$IN_6 = s_6 - s_7 - s_{11}$	$IN_{22} = 2s_3 + 2s_7 + 2s_{11} - s_{13}$
$IN_7 = s_7 - s_8 - s_{10}$	$IN_{23} = 2s_3 + 2s_6 - s_{13}$
$IN_8 = s_8 - s_9$	$IN_{24} = s_3 - s_5 + s_{11}$
$IN_9 = 2s_{12} - s_{13}$	$IN_{25} = 2s_2 + 2s_9 + 2s_{10} + 2s_{11} - s_{13}$
$IN_{10} = s_7 - s_9 - s_{10}$	$IN_{26} = 2s_2 + 2s_8 + 2s_{10} + 2s_{11} - s_{13}$
$IN_{11} = s_6 - s_9 - s_{10} - s_{11}$	$IN_{27} = 2s_2 + 2s_7 + 2s_{11} - s_{13}$
$IN_{12} = s_6 - s_8 - s_{10} - s_{11}$	$IN_{28} = 2s_2 + 2s_6 - s_{13}$
$IN_{13} = 2s_5 + 2s_8 + 2s_{10} - s_{13}$	$IN_{29} = s_2 - s_5 + s_{11}$
$IN_{14} = 2s_5 + 2s_7 - s_{13}$	$IN_{30} = s_2 - s_4 + s_{11}$
$IN_{15} = 2s_5 + 2s_6 - 2s_{11} - s_{13}$	$IN_{31} = 2s_1 - s_{13}$
$IN_{16} = 2s_4 + 2s_9 + 2s_{10} - s_{13}$	$IN_{32} = s_1 - s_{12}$
Terminal nodes	
$TN_1 = OR - s_1$	$TN_2 = 2OR - s_{13}$
$TN_3 = OR - s_{12}$	

OR, is an appropriate full route, labeled here as FR_1. A direct ER for this system, involves no more than $q + 2 = 9 + 2 = 11$ elementary steps, most involving far fewer. Thus, from Table 1, we can identify the following three ERs or cycles via inspection labeled here as

ER_1: $s_2 + s_3 - s_6 - s_{11} = 0$;

ER_2: $s_4 + s_5 - s_7 - s_{10} + s_{11} = 0$ and

ER_3: $s_8 + s_9 - s_{10} = 0$.

It can be seen that this set of 4 RRs (1 FR and 3 ERs) comprises all reaction steps and is, thus, an adequate independent set. Next, the direct INs are stoichiometrically enumerated based on the QSS of the linearly independent intermediate species (Table 2) [13–15]. By definition, a direct QSS condition at a node involves no more than $p - (q - 1) = 13 - 9 + 1 = 5$ rates and can be obtained by linearly combining Qs listed in Table 2. In other words, the degree of INs is $\leqslant 5$. Clearly Q_6 does not satisfy this criterion. An appropriate set of INs may be obtained by linearly combining those listed in Table 2. This is necessary, since it is not known a priori which nodes will be needed for construction of the RR graph. A complete set of INs by linear combination of those in Table 2 is listed in Table 3. The TNs, similarly are enumerated based on the QSS of the terminal species [13–15]. The complete list of hence enumerated INs and TNs is presented in Table 3. The alternate stoichiometric algorithm is described by us [13–15].

5. RR graph construction

Once, the list of the linearly independent RRs (1 FR and 3 ERs) and nodes (INs and TNs) for the system is determined as described above or via stoichiometric algorithms, the next step in our procedure is to construct the graph-theoretic RR graph, on which each reaction step s_ρ is drawn as a directed branch, showing assumed direction, while the nodes represent reaction connectivity, such that all the remaining FRs and ERs can be visualized on the graph as walks or paths. One starts with the construction of the RR graph based on the 4 linearly independent RRs, i.e., ER_1, ER_2, ER_3 and FR_1. The ERs are first assembled into what is called a cycle graph (Fig. 1A). For instance, ER_1 and ER_2 have step s_{11} in common, and, may thus be combined (Fig. 1A). ER_2 and ER_3 have step s_{10} in common and may thus be fused resulting in the cycle graph. Next, the adsorption/desorption steps, i.e., s_1, s_{12} and s_{13} which are not involved in any of the ER, are added to the cycle graph such that FR_1 may be traced as a walk on the network.

While seemingly straightforward, the last step is actually rather tricky due to the fact that non-unit stoichiometric numbers are present in the FRs [15]. This is, in fact, characteristic of most catalytic reactions. Thus s_{13} must occur twice on the RR graph. Further, the addition of these steps to the cycle graph must be done such that all nodes are among the INs. It is, further, seen from Table 3 that the INs for s_{13} all involve doubled other steps, e.g., (IN_5) n_5: $2s_5 + 2s_9 + 2s_{10} - s_{13} = 0$. Moreover, since the step s_{13} is involved twice in FR_1, the two steps s_{13} should appear in the network in series. This is so because the mass balance conditions of the terminal species, CH_3OH, CO and H_2, require the rates of the desorption/adsorption steps to satisfy the condition $2r_1 = 2r_{12} = r_{13} = 2r_{OR}$ (Table 2). Because of these constraints, all of the steps (including the OR) must be doubled, i.e., two identical steps in parallel between two given nodes. This is readily accomplished by fusing together two cycle graphs shown in Fig. 1A and adding the remaining steps as depicted in Fig. 1. It can be checked that all the nodes are among the enumerated INs and TNs. Thus, the final RR graph for methanol decomposition is shown in Fig. 1B.

It may be noted that all reaction steps are present twice in the RR graph. This is, in fact, a general property of balanced RR graphs, i.e., the mass balance conditions require every step in a RR network, including the ORs, to be present in the network an equal number of times, in this case 2, because of the particular stoichiometry. The final RR network thus assembled is shown in Fig. 1B. Upon inspection of this graph, it is seen that all nodes are balanced in that they satisfy the quasi-state condi-

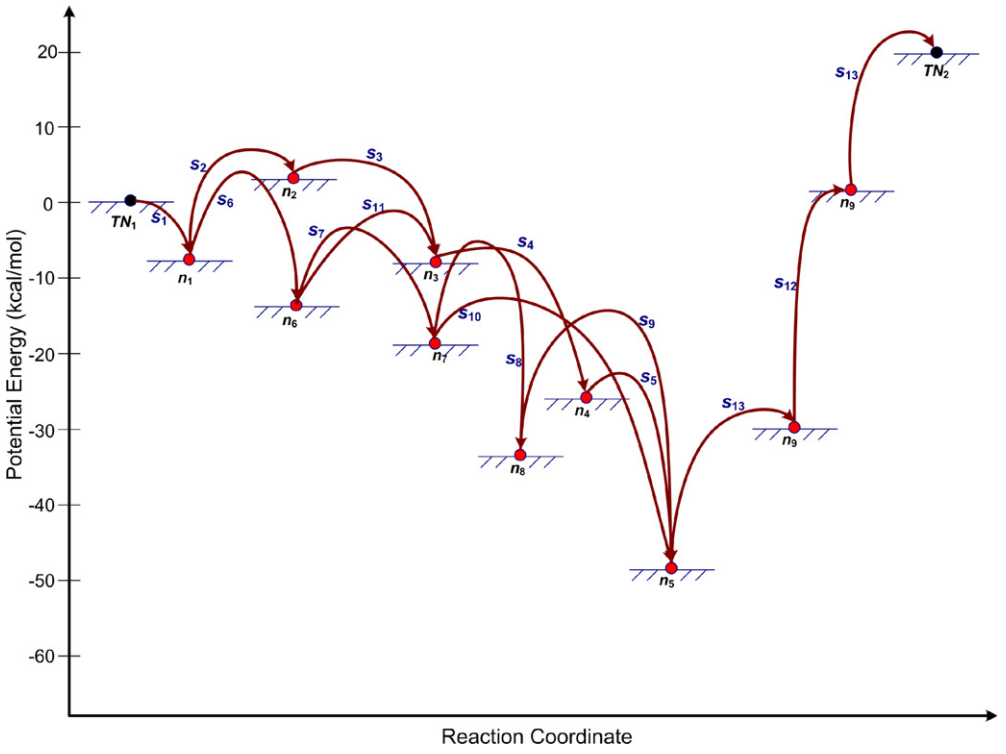

Fig. 2. Energy diagram corresponding to the RR graph for methanol decomposition reaction on Pt(111).

Table 4
Stoichiometrically distinct direct FRs and ERs for methanol decomposition reaction

Reaction route	Expression
	Full RRs
FR_1 (Path 1)	$s_1+s_2+s_3+s_4+s_5+s_{12}+2s_{13}=\text{OR}$ $CH_3OH \rightarrow CH_3O \rightarrow CH_2O \rightarrow CHO \rightarrow CO$
FR_2 (Path 2)	$s_1+s_6+s_7+s_8+s_9+s_{12}+2s_{13}=\text{OR}$ $CH_3OH \rightarrow CH_2OH \rightarrow CHOH \rightarrow COH \rightarrow CO$
FR_3 (Path 3)	$s_1+s_6+s_7+s_{10}+s_{12}+2s_{13}=\text{OR}$ $CH_3OH \rightarrow CH_2OH \rightarrow CHOH \rightarrow CO$
FR_4 (Path 4)	$s_1+s_2+s_3-s_{11}+s_7+s_8+s_9+s_{12}+2s_{13}=\text{OR}$ $CH_3OH \rightarrow CH_3O \rightarrow CH_2O \rightarrow CH_2OH \rightarrow CHOH \rightarrow COH \rightarrow CO$
FR_5 (Path 5)	$s_1+s_2+s_3-s_{11}+s_7+s_{10}+s_{12}+2s_{13}=\text{OR}$ $CH_3OH \rightarrow CH_3O \rightarrow CH_2O \rightarrow CH_2OH \rightarrow CHOH \rightarrow CO$
FR_6 (Path 6)	$s_1+s_6+s_{11}+s_4+s_5+s_{12}+2s_{13}=\text{OR}$ $CH_3OH \rightarrow CH_2OH \rightarrow CH_2O \rightarrow CHO \rightarrow CO$
	Empty RRs
ER_1	$s_2+s_3-s_6-s_{11}=0$
ER_2	$s_4+s_5-s_7-s_{10}+s_{11}=0$
ER_3	$s_8+s_9-s_{10}=0$
ER_4	$s_2+s_3+s_4+s_5-s_6-s_7-s_8-s_9=0$
ER_5	$s_4+s_5-s_7-s_8-s_9+s_{11}=0$
ER_6	$s_2+s_3+s_4+s_5-s_6-s_7-s_{10}=0$

tions of surface intermediates. The topological enumeration of all reaction pathways or RRs can now be easily accomplished by tracing walks on the RR graph topology. A total of 6 direct FRs can be easily traced as walks between the terminal nodes, and 6 direct ERs can be traced as cycles. Of course, only $p-q=13-9=4$ FRs are linearly independent, i.e., the others can be resulted by their linear combination. The complete list of thus generated FRs and ERs is listed in Table 4. It must be noted that exactly the same set of direct RRs (FRs and ERs) can be generated based on our stoichiometric algorithm [13–15]. Thus, topological enumeration of FRs and ERs is an effective alternate to stoichiometric enumeration [19].

Amongst the enumerated FRs, three FRs are initiated via O–H cleavage (Paths 1, 4 and 5), whilst the rest start via C–H cleavage of adsorbed methanol (Paths 2, 3 and 6). From among these, Paths 1, 3 and 6 have been identified by Greeley and Mavrikakis [6] and Gokhale et al. [17]. On the other hand, Paths 1, 2 and 6 have been identified by Neurock and coworkers [7,28]. Further, Paths 2 and 6 were proposed by Bagotzky et al. [29]. Kua and Goddard [8] and Ishikawa et al. [9] have recognized Path 2. However, Paths 4 and 5 for methanol decomposition have apparently not so far been identified in the literature. Clearly, rigorous enumeration of FRs as done here is essential. Of course, not all FRs may contribute significantly towards the total flux of the OR. The dominant FRs can be identified readily using the RR circuit approach as described next.

The RR graph can also be used to directly generate appropriate energy diagrams, as shown in Fig. 2. As mentioned above, each node is characterized by a potential energy or enthalpy on the diagram. Thus, each plateau corresponds to the respective node on the RR graph. In addition to reaction enthalpy or the difference between its nodes, the energy diagram also depicts both the forward and reverse activation energies for each elementary step (Table 1). The FRs and ERs are evident on the energy diagram as well.

6. Reaction network, thermodynamics, and kinetics

Each cycle or ER in the RR graph is subject to KPL via Eq. (2). As an example of KPL, consider ER_1, i.e., $s_2 + s_3 - s_6 - s_{11} = 0$. The corresponding linear combination of affinities is, of course, equal to zero

$$A_2 + A_3 - A_6 - A_{11} = 0, \quad \text{i.e.,}$$

$$\left(\frac{\vec{r}_2}{\overleftarrow{r}_2}\right)\left(\frac{\vec{r}_3}{\overleftarrow{r}_3}\right)\left(\frac{\overleftarrow{r}_6}{\vec{r}_6}\right)\left(\frac{\overleftarrow{r}_{11}}{\vec{r}_{11}}\right) = 1. \tag{12}$$

Since in a cycle, the species activities cancel out, we have a thermodynamic consistency check on the predicted rate constants of steps in a cycle, i.e.,

$$\frac{\vec{k}_2}{\overleftarrow{k}_2}\frac{\vec{k}_3}{\overleftarrow{k}_3}\frac{\overleftarrow{k}_6}{\vec{k}_6}\frac{\overleftarrow{k}_{11}}{\vec{k}_{11}} = 1 = K_2 K_3 K_6^{-1} K_{11}^{-1}. \tag{13}$$

The calculated rate constants must be consistent with these constraints. There are two other such constraints for the remaining two independent ERs. Alternatively, not all rate constants need to be predicted, some may be found from KPL relations.

Furthermore, the affinities, A_ρ of the elementary reactions ($A_\rho = -\Delta G_\rho$), in a FR are interrelated with the affinity of the OR, A_{OR}, via similar KPL relation. For instance, for

$$FR_1: \quad s_1 + s_2 + s_3 + s_4 + s_5 + s_{12} + 2s_{13},$$

we have

$$A_1 + A_2 + A_3 + A_4 + A_5 + A_{12} + 2A_{13} = A_{OR}, \quad \text{i.e.,}$$
$$K_1 K_2 K_3 K_4 K_5 K_{12} K_{13}^2 = K_{OR}, \tag{14}$$

where K_ρ and K_{OR} is the equilibrium constant of the elementary reaction step s_ρ and OR respectively. The data in Table 1 are consistent with this.

Each node follows KCL, as given by Eq. (1). Thus, KPL ensures thermodynamic consistency while KCL is used to rigorously determine the network kinetics. For the case of methanol decomposition, the following equations result as per the application of KCL at the 9 linearly independent nodes, i.e. (Fig. 1),

$$\begin{aligned}
&n_1: \quad r_1 - r_2 - r_6 = 0; \quad n_2: \quad r_2 - r_3 = 0;\\
&n_3: \quad r_3 - r_4 + r_{11} = 0; \quad n_4: \quad r_4 - r_5 = 0;\\
&n_5: \quad 2r_5 + 2r_9 + 2r_{10} - r_{13} = 0;\\
&n_6: \quad r_6 - r_7 - r_{11} = 0; \quad n_7: \quad r_7 - r_8 - r_{10} = 0;\\
&n_8: \quad r_8 - r_9 = 0; \quad \text{and} \quad n_9: \quad r_{13} - 2r_{12} = 0
\end{aligned} \tag{15}$$

which provide the network constraints on the rates of elementary steps. Using mass action kinetics, these KCL equations reduce to the following set

$$\begin{aligned}
&\left(\vec{k}_1 p_{CH_3OH}\theta_0 - \overleftarrow{k}_1\theta_{CH_3OH\cdot S}\right)\\
&\quad - \left(\vec{k}_2\theta_{CH_3OH\cdot S}\theta_0 - \overleftarrow{k}_2\theta_{CH_3O\cdot S}\theta_{H\cdot S}\right)\\
&\quad - \left(\vec{k}_6\theta_{CH_3OH\cdot S}\theta_0 - \overleftarrow{k}_6\theta_{CH_2OH\cdot S}\theta_{H\cdot S}\right) = 0,\\
&\left(\vec{k}_2\theta_{CH_3OH\cdot S}\theta_0 - \overleftarrow{k}_2\theta_{CH_3O\cdot S}\theta_{H\cdot S}\right)\\
&\quad - \left(\vec{k}_3\theta_{CH_3O\cdot S}\theta_0^2 - \overleftarrow{k}_3\theta_{CH_2O\cdot S_2}\theta_{H\cdot S}\right) = 0,\\
&\left(\vec{k}_3\theta_{CH_3O\cdot S}\theta_0^2 - \overleftarrow{k}_3\theta_{CH_2O\cdot S_2}\theta_{H\cdot S}\right)\\
&\quad - \left(\vec{k}_4\theta_{CH_2O\cdot S_2} - \overleftarrow{k}_4\theta_{CHO\cdot S}\theta_{H\cdot S}\right)\\
&\quad + \left(\vec{k}_{11}\theta_{CH_2OH\cdot S}\theta_0^2 - \overleftarrow{k}_{11}\theta_{CH_2O\cdot S_2}\theta_{H\cdot S}\right) = 0,\\
&\left(\vec{k}_4\theta_{CH_2O\cdot S_2} - \overleftarrow{k}_4\theta_{CHO\cdot S}\theta_{H\cdot S}\right)\\
&\quad - \left(\vec{k}_5\theta_{CHO\cdot S}\theta_0 - \overleftarrow{k}_5\theta_{CO\cdot S}\theta_{H\cdot S}\right) = 0,\\
&2\left(\vec{k}_5\theta_{CHO\cdot S}\theta_0 - \overleftarrow{k}_5\theta_{CO\cdot S}\theta_{H\cdot S}\right)\\
&\quad + 2\left(\vec{k}_9\theta_{COH\cdot S}\theta_0 - \overleftarrow{k}_9\theta_{CO\cdot S}\theta_{H\cdot S}\right)\\
&\quad + 2\left(\vec{k}_{10}\theta_{CHOH\cdot S}\theta_0^2 - \overleftarrow{k}_{10}\theta_{CO\cdot S}\theta_{H\cdot S}^2\right)\\
&\quad - \left(\vec{k}_{13}\theta_{H\cdot S}^2 - \overleftarrow{k}_{13}p_{H_2}\theta_0^2\right) = 0,\\
&\left(\vec{k}_6\theta_{CH_3OH\cdot S}\theta_0 - \overleftarrow{k}_6\theta_{CH_2OH\cdot S}\theta_{H\cdot S}\right)\\
&\quad - \left(\vec{k}_7\theta_{CH_2OH\cdot S}\theta_0 - \overleftarrow{k}_7\theta_{CHOH\cdot S}\theta_{H\cdot S}\right)\\
&\quad - \left(\vec{k}_{11}\theta_{CH_2OH\cdot S}\theta_0^2 - \overleftarrow{k}_{11}\theta_{CH_2O\cdot S_2}\theta_{H\cdot S}\right) = 0,\\
&\left(\vec{k}_7\theta_{CH_2OH\cdot S}\theta_0 - \overleftarrow{k}_7\theta_{CHOH\cdot S}\theta_{H\cdot S}\right)\\
&\quad - \left(\vec{k}_8\theta_{CHOH\cdot S}\theta_0 - \overleftarrow{k}_8\theta_{COH\cdot S}\theta_{H\cdot S}\right)\\
&\quad - \left(\vec{k}_{10}\theta_{CHOH\cdot S}\theta_0^2 - \overleftarrow{k}_{10}\theta_{CO\cdot S}\theta_{H\cdot S}^2\right) = 0,\\
&\left(\vec{k}_8\theta_{CHOH\cdot S}\theta_0 - \overleftarrow{k}_8\theta_{COH\cdot S}\theta_{H\cdot S}\right)\\
&\quad - \left(\vec{k}_9\theta_{COH\cdot S}\theta_0 - \overleftarrow{k}_9\theta_{CO\cdot S}\theta_{H\cdot S}\right) = 0,\\
&\left(\vec{k}_{13}\theta_{H\cdot S}^2 - \overleftarrow{k}_{13}p_{H_2}\theta_0^2\right) - 2\left(\vec{k}_{12}\theta_{CO\cdot S} - \overleftarrow{k}_{12}p_{CO}\theta_0\right) = 0.
\end{aligned} \tag{16}$$

The above set of 9 non-linear algebraic KCL equations, along with the site balance equation,

$$\begin{aligned}
&\theta_{CH_3OH\cdot S} + \theta_{CH_2OH\cdot S} + \theta_{CH_3O\cdot S} + \theta_{CH_2O\cdot S_2} + \theta_{CHOH\cdot S}\\
&\quad + \theta_{CHO\cdot S} + \theta_{COH\cdot S} + \theta_{CO\cdot S} + \theta_{H\cdot S} + \theta_0 = 1
\end{aligned} \tag{17}$$

may be numerically solved simultaneously, for given input conditions (temperature and partial pressures of reactants) and conversion, to obtain the unknown site fractions of intermediate species, θ_k. Thereupon, one may readily calculate the rate, affinity and resistance of each elementary reaction step. Finally, the rate of the overall reaction may be obtained from the TNs, e.g., $r_{OR} = r_1 = r_{12} = r_{13}/2$ (Fig. 1). Moreover, if combined with mass-balance conditions for a given reactor, one can predict the reactor performance. This procedure is distinct from conventional microkinetic analysis [17], wherein differential equations for a given reactor are solved numerically to obtain conversion, from which rate of a reaction is inferred indirectly.

Finally, once the step resistances are calculated, the elimination of parallel routes with higher "resistance" and identification of steps with highest resistance in a sequence as rate limiting steps (RLS) can be accomplished rigorously and transparently, as described next.

7. Network analysis and pruning

As a first approximation, as is commonly done, the most favorable reaction routes may be identified based on the energetic considerations by simply comparing the energy diagrams of the

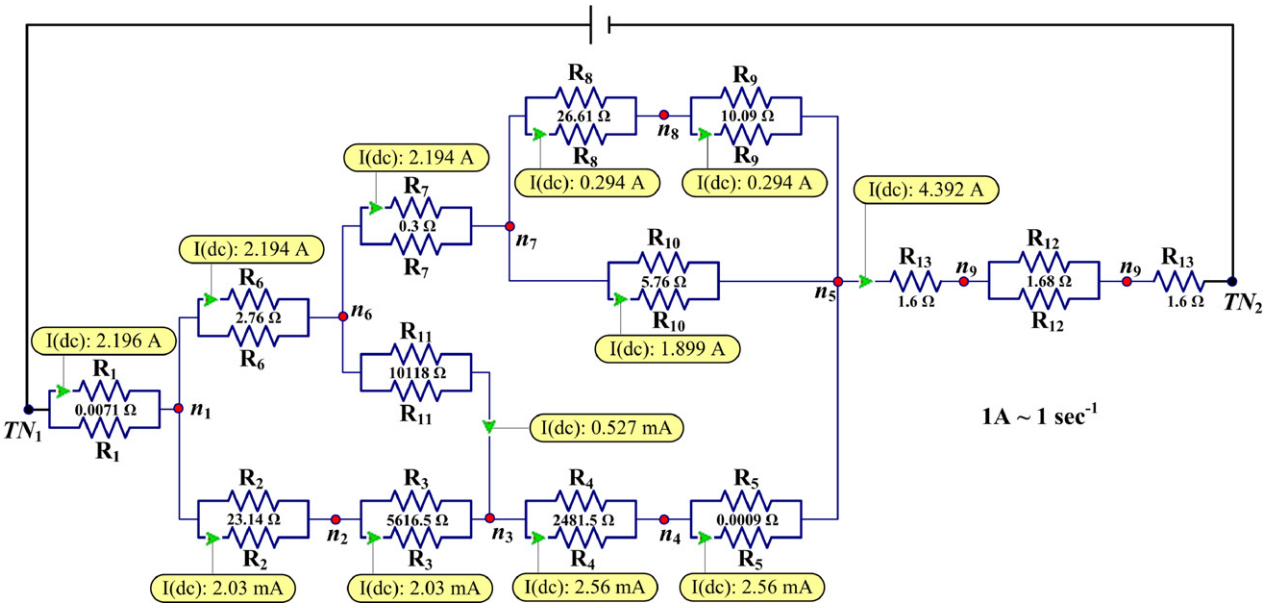

Fig. 3. Reaction circuitry/electrical analog of the RR graph for methanol decomposition reaction. The branch currents represent the TOFs (s^{-1}) for the corresponding elementary steps on Pt(111) at 553 K, 1 atm and 1% methanol in feed, PFR $W/F = 100$ s.

various pathways (Fig. 2). For instance, one may expect pathways involving step s_2 to be less favorable than those involving s_6. In other words, the initial dehydrogenation step is indicated to proceed via the C–H cleavage of adsorbed methanol to yield hydroxymethyl ($CH_2OH{\cdot}S$) in preference to the O–H cleavage producing methoxide ($CH_3O{\cdot}S$) on Pt(111), owing to the higher activation energy barrier for step s_2. However, such qualitative arguments can lead to erroneous conclusions because the rate of a step depends not only upon the energy barrier but also on concentration of the reactants. Further, flux along a pathway may not be determined by a single RLS.

A more accurate and robust simplification and reduction may be accomplished based on a comparison of the flux (current) along different pathways in the reaction circuit or via a comparison of pathway resistance (Fig. 3). As mentioned above, being consistent, RR graphs can be directly converted into an equivalent electric circuit, or wiring diagram allowing use of the gamut of techniques available for electric circuit analysis. For the methanol decomposition example, the equivalent electrical circuit can be obtained simply by replacing the branches in Fig. 1B by the step resistances. Fig. 3, thus, provides the electrical analog or the reaction circuit of the methanol decomposition. The branch currents in Fig. 3, simulated using Multisim software, a schematic simulation and programmable logic tool produced by Electronics Workbench [30], as an alternate to the above mentioned KCL approach, represent the turnover frequencies (TOFs, s^{-1}) for the corresponding elementary steps on Pt(111) simulated in a plug flow reactor (PFR) with $W/F = 100$ s at 553 K, 1 atm and 1% methanol in feed. First of all note that KCL is followed at all nodes. Fig. 3 is a very revealing diagram, from which many important conclusions regarding the network may be drawn via an inspection of branch currents, current splitting at nodes, and a comparison of resistances. The total current is 4.4 A ($2r_{OR} = 4.4\ s^{-1}$) under these conditions, split equally between two parallel s_1. At n_1, it is seen that the current (flux) flows almost entirely through the upper branch (s_6), even though R_6 is only an order of magnitude lower than R_2. This is because of a very large R_3 in series with R_2. Thus, the O–H cleavage pathway contributes virtually nothing to the overall methanol decomposition pathway under these conditions. The upper branch (C–H cleavage pathway) splits again at node n_6. Again, due to the large difference in R_7 and R_{11}, the flux through the upper branch dominates. A further split occurs at n_7. Here, while almost 90% of the flux is through lower branch (R_{10}), the upper branch ($R_8 + R_9$) contribution (about 10%) cannot be neglected. It can be readily seen that steps s_8 and s_9 are an order of magnitude lower than step s_{10}, a conclusion similar to that of Gokhale et al. [17] and Kandoi et al. [16] based on their microkinetic analysis. It can further be seen from Fig. 3 that Path 3, i.e. $s_1 + s_6 + s_7 + s_{10} + s_{12} + 2s_{13}$, ($CH_3OH \rightarrow CH_2OH \rightarrow CHOH \rightarrow CO$) is the dominant reaction pathway for these typical reaction conditions, since majority of the current (flux) flows through this pathway. However, the parallel pathway, FR_2 comprising of steps s_8 and s_9, also contributes non-negligibly.

To further, confirm these findings, detailed comparison of the resistances is called for under a variety of conditions along parallel paths so that irrefutable conclusions can be made about the mechanism and kinetics of methanol decomposition. This is most readily accomplished by a comparison of resistances of the two parallel pathways between two given nodes, which have the same affinity drop by virtue of KPL, i.e., by considering each ER as two parallel paths and comparing the total resistance of each path for the submechanism between two nodes. If the resistance along one path is much larger than the other, it would be safe to assume that the path contributes little to the flux and may be neglected.

As an example, consider ER_3, i.e., let us compare the resistances along parallel pathways between nodes n_7 and n_5, namely, the two parallel paths that produce CO·S species. In

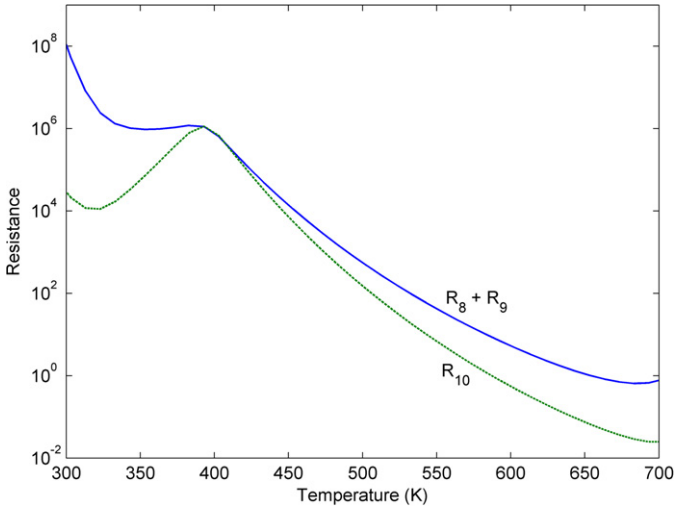

Fig. 4. R_{10} vs $R_8 + R_9$, as a function of temperature for methanol decomposition reaction on Pt(111) (1% methanol in feed, 1 atm, PFR with $W/F = 100$ s).

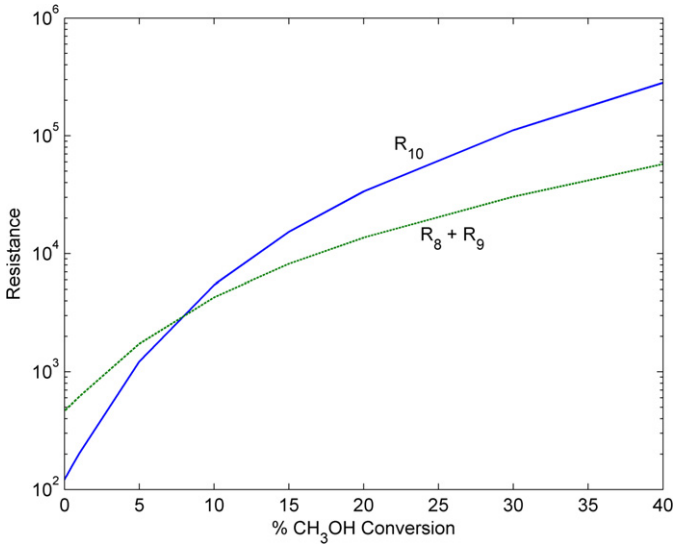

Fig. 5. R_{10} vs $R_8 + R_9$, as a function of conversion at $T = 503$ K for methanol decomposition reaction on Pt(111) (1% methanol in feed, 1 atm).

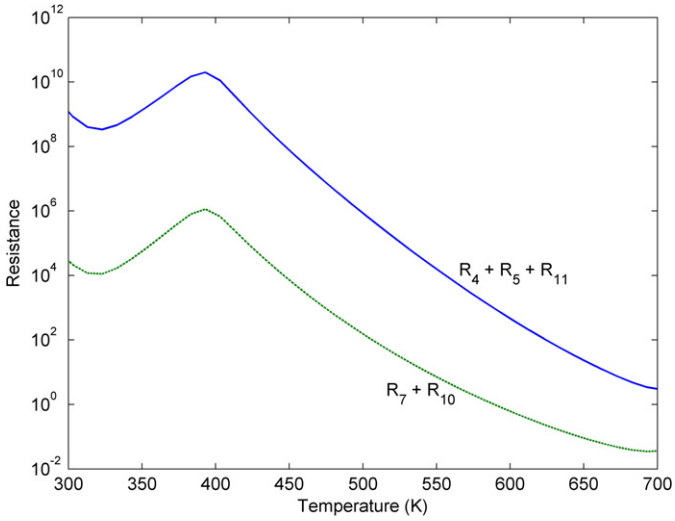

Fig. 6. $R_4 + R_5 + R_{11}$ vs $R_7 + R_{10}$ as a function of temperature for methanol decomposition reaction on Pt(111) (1% methanol in feed, 1 atm, PFR with $W/F = 100$ s).

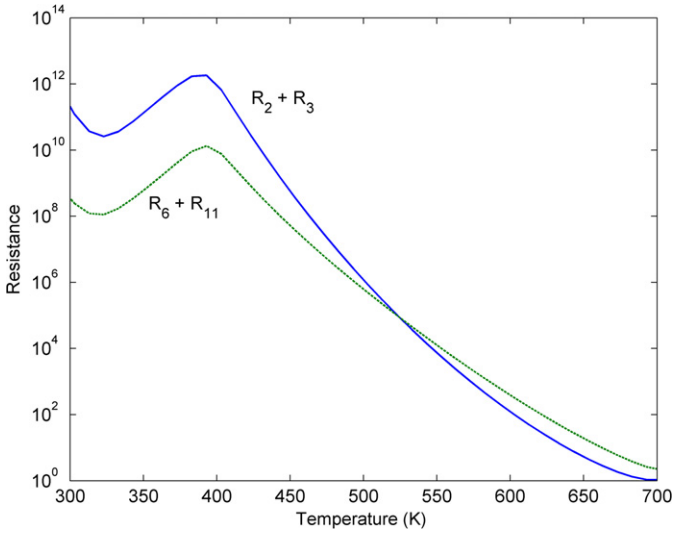

Fig. 7. $R_2 + R_3$ vs $R_6 + R_{11}$, as a function of temperature for methanol decomposition reaction on Pt(111) (1% methanol in feed, 1 atm, PFR with $W/F = 100$ s).

the first path, i.e. s_{10}, CHOH·S directly decomposes into CO·S, where as in the second path, i.e., $s_8 + s_9$, COH·S is first formed, which then decomposes into CO·S. The first path consists of a single resistance, R_{10} while the second path consists of two resistances in series, R_8 and R_9, the overall resistance being $R_8 + R_9$. To compare these two parallel paths for this submechanism under a broad range of conditions, these resistances as a function of temperature are shown in Fig. 4. $R_8 + R_9$ is found to have a higher resistance than R_{10} in the entire temperature range, except around 400–425 K, for the considered reaction conditions. Although, as can be seen from Fig. 3, flux through s_8 and s_9 is only about 10% of the total flux, it is clear that deletion of s_8 and s_9 is not justifiable. To further investigate this, the effect of composition of terminal species on path resistance is investigated. Fig. 5, thus, compares the resistance of these two parallel paths to produce CO·S species in ER_3 at a temperature of 503 K as a function of methanol conversion. It can be seen that for conversion <10%, direct decomposition of CHOH·S to CO·S is the dominant reaction pathway, while at higher conversion, CHOH·S first decomposes to COH·S and then to CO·S. A similar analysis at $T = 553$ K, shows FR_3 to be a dominant reaction pathway for conversions <75% while at higher conversions, FR_2 is the dominant reaction pathway. Thus, both FR_2 and FR_3 are significant depending upon the reaction conditions, and the parallel pathways via s_{10} and, s_8 and s_9, are hence retained in the pruned mechanism.

Similar comparisons for ER_2, i.e., $s_4 + s_5 - s_7 - s_{10} + s_{11} = 0$, and ER_1, i.e., $s_2 + s_3 - s_6 - s_{11} = 0$, are shown in Figs. 6 and 7, respectively. Thus, pathways involving steps s_2, s_3, s_4, s_5 and s_{11} are unlikely, although from Fig. 7 it seems that, the pathway proceeding via steps s_2 and s_3, i.e. initial O–H cleavage of adsorbed methanol begins to contribute more at temperatures

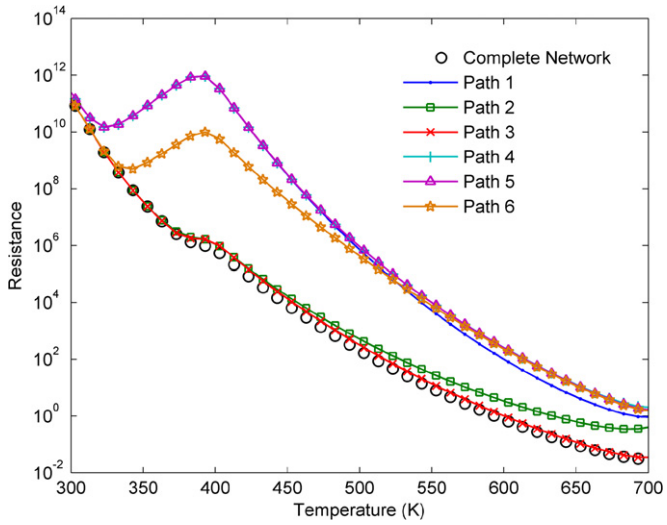

Fig. 8. Comparison of the path resistance with the overall network resistance (1% methanol in feed, 1 atm, PFR with $W/F = 100$ s).

above 525 K. However, the subsequent steps for the pathway via initial O–H cleavage of adsorbed methanol, say ($s_4 + s_5$) have much higher resistance than steps involved in the pathway via initial C–H cleavage of adsorbed methanol, say ($s_7 + s_{10}$). Thus, s_2, s_3, s_4, s_5 and s_{11} may be dropped from the mechanism.

A third way of network pruning is to evaluate the overall resistance of the network. Then, the FRs or steps whose resistance has no effect on the overall resistance of the network could be disregarded. The overall network resistance of the reaction circuit shown in Fig. 3 was evaluated from individual elementary reaction step resistances, using conventional electrical circuit theory [31].

A comparison among the individual path resistances and the overall resistance of the entire network is shown in Fig. 8. It is seen that the resistance along Path 3, i.e. FR_3 compares well with the overall resistance of the network, while the resistance of all other paths, with the exception of Path 2, is significantly higher, suggesting FR_3 and FR_2 as dominant parallel reaction pathways for methanol decomposition reaction on Pt(111) under the conditions considered in this study. Even if all of the FRs, excepting FR_3 and FR_2, are eliminated, the overall resistance of the network still remains largely unaffected, as is the rate of the overall reaction. It must be noted that reaction steps s_2, s_3, s_4, s_5 and s_{11} are not involved in FR_3 and FR_2 (Table 4) and, consequently this analysis also justifies their elimination from the reaction mechanism, resulting into a 8 step simplified reaction network for methanol decomposition on Pt(111), as shown in Fig. 9.

Finally, to further validate the elimination of steps s_2, s_3, s_4, s_5 and s_{11}, we checked the effect of neglecting these steps on the overall kinetics by comparing the simulated overall rate of the 13-step mechanism (Table 1) to the mechanism less s_2, s_3, s_4, s_5 and s_{11}. As seen in Fig. 10, the elimination of steps s_2, s_3, s_4, s_5 and s_{11} (simplified 8 step mechanism) does not materially affect the overall kinetics. Moreover, as can be seen from Fig. 10, FR_2 does contribute to the net rate non-negligibly, and must be retained in the reduced network. It is noteworthy that all of the eliminated steps are based on the initial O–H bond scission pathway. It is, thus, clear that this is not a significant pathway in methanol decomposition on Pt(111).

This pruned network shows that the initial dehydrogenation step for methanol is via step s_6, i.e., via initial C–H cleavage of adsorbed methanol. The O–H cleavage pathway plays little or no role in the overall methanol decomposition on

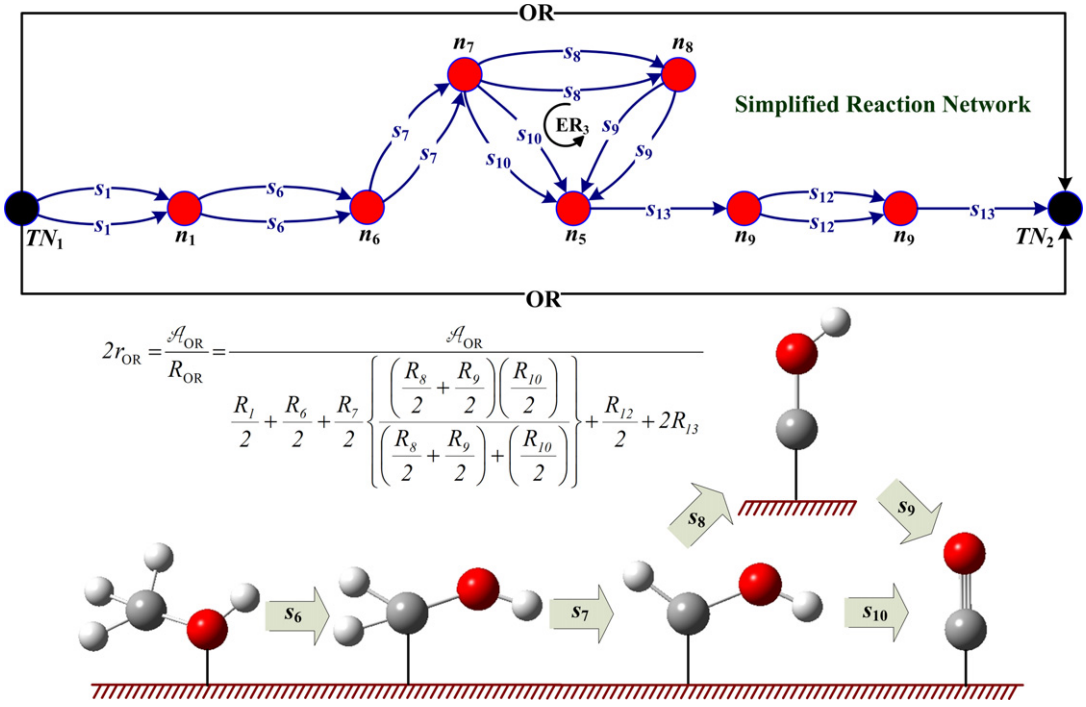

Fig. 9. Simplified reaction network and schematic of the dominant reaction pathways for methanol decomposition reaction on Pt(111).

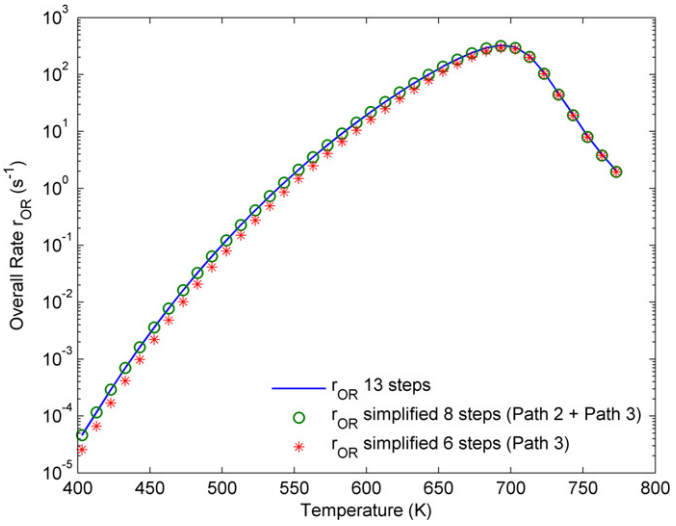

Fig. 10. Comparison of overall mechanism kinetics with and without s_2, s_3, s_4, s_5 and s_{11} (1% methanol in feed, 1 atm, PFR with $W/F = 100$ s).

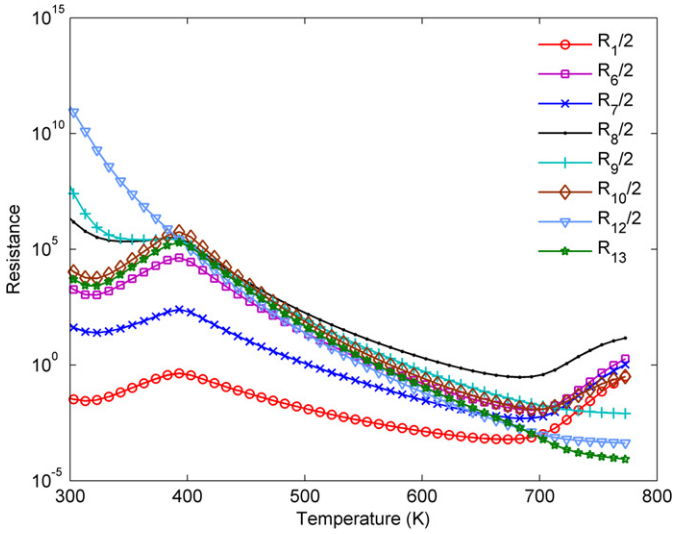

Fig. 11. Determination of RLS by comparing the series resistances in the reduced RR network (1% methanol in feed, 1 atm, PFR with $W/F = 100$ s).

Pt(111), which agrees with the experimental and theoretical findings of several researchers. To the authors' knowledge, no direct spectroscopic evidence for methoxide species on clean Pt(111) has been reported in the literature except for Peck et al. [32], who detected methoxide species on clean Pt(111) by using a methyl nitrite precursor. Quantum chemical calculations performed over platinum clusters also suggest that methanol prefers to dehydrogenate by the activation of its C–H rather than O–H bond [8,9]. Franaszczuk et al. [33] have experimentally concluded the first step to be the C–H scission of methanol on platinum clusters in electrochemical environment. Recently, Desai et al. [28], based on nonlocal gradient corrected periodic DFT calculations, have also reported the methanol decomposition pathway involving an initial activation of C–H bond to be thermodynamically more favorable than O–H bond activation on Pt(111). The model predictions by Greeley and Mavrikakis [6] based on DFT analysis suggest that the adsorbed hydroxymethyl, product of the C–H bond activation is ∼0.8 eV more stable than the adsorbed methoxy, product of the O–H bond activation on Pt(111). Furthermore, Gokhale et al. [17] also show that the net rate of step s_6 is higher than that of step s_2, with a similar conclusion. The experimental findings by Kandoi et al. [16] coupled with microkinetic modeling using DFT, suggests FR_3 to be a dominant reaction pathway for methanol decomposition on Pt(111) which is in accord with our findings based on our graph-theoretic approach, although we find that in addition FR_2 must be retained.

Finally, the rate limiting steps (RLS) may be identified by comparing the series step resistances, wherein the step with the highest resistance would govern the reaction kinetics and is the RLS. Fig. 3 indicates that s_8, s_9 and s_{10} are the RLSs under the reaction conditions of Fig. 3. To further investigate this, Fig. 11 evaluates the resistance of the reaction steps at other temperatures. It is seen that, in the temperature range of 300–400 K, step s_{12} is the RLS. In the temperature range, 400–500 K, steps s_8, s_9 and s_{10}, are the slowest. While at temperature above 500 K, step s_8 is the RLS. Thus, it is clear that it is not possible to further reduce this mechanism down to a single RLS under all conditions.

8. Conclusions

This paper illustrates our new graph-theoretic approach, called the reaction route (RR) graph approach, to analyze complex catalytic reaction mechanisms, kinetics, and pathways within a comprehensive and consistent framework, based on first principles predictions of reaction kinetics and thermodynamics. In addition to its intuitive appeal in depicting reaction pathways as walks or paths, the RR graph can be directly converted into an equivalent reaction circuit, clearly showing flux in all the parallel pathways and providing step resistances for a quantitative pruning of the network to retain the dominant pathways and identify any rate limiting steps.

The application of the RR graph approach to methanol decomposition on Pt(111) shows two dominant reaction pathways, FR_3 and FR_2 (Table 4) depending upon the reaction conditions, both with an initial C–H bond activation of methanol over Pt(111). Thus, the reaction proceeds exclusively via an initial dehydrogenation of the C–H bond rather than through the O–H bond of methanol. As this example of methanol decomposition shows, the RR network approach is a valuable new weapon in the arsenal of the catalytic scientist.

References

[1] A. Groß, Surf. Sci. 500 (2002) 347.
[2] M. Neurock, J. Catal. 216 (2003) 73.
[3] F. Ruette, M. Sanchez, A. Sierraalta, C. Mendoza, R. Anez, L. Rodriguez, O. Lisboa, J. Daza, P. Manrique, Z. Perdomo, M. Rosa-Brussin, J. Mol. Catal. A Chem. 228 (2005) 211.
[4] L.J. Broadbelt, J. Pfaendtner, AIChE J. 51 (2005) 2112.
[5] J. Greeley, M. Mavrikakis, J. Am. Chem. Soc. 124 (2002) 7193.
[6] J. Greeley, M. Mavrikakis, J. Am. Chem. Soc. 126 (2004) 3910.
[7] D. Cao, G.-Q. Lu, A. Wieckowski, S.A. Wasileski, M. Neurock, J. Phys. Chem. B 109 (2005) 11622.
[8] J. Kua, W.A. Goddard III, J. Am. Chem. Soc. 121 (1999) 10928.

[9] Y. Ishikawa, M. Liao, C. Cabrera, Surf. Sci. 463 (2000) 66.
[10] A.T. Balaban, in: D. Bonchev, O. Mekenyan (Eds.), Graph Theoretical Approaches to Chemical Reactivity, Kluwer Academic, Dordrecht, 1994, p. 137.
[11] O.N. Temkin, A.V. Zeigarnik, D.G. Bonchev, Chemical Reaction Networks: A Graph-Theoretical Approach, CRC Press, New York, 1996.
[12] N. Balabanian, T. Bickart, Electrical Network Theory, Wiley, New York, 1969.
[13] I. Fishtik, C.A. Callaghan, R. Datta, J. Phys. Chem. B 108 (2004) 5671.
[14] I. Fishtik, C.A. Callaghan, R. Datta, J. Phys. Chem. B 108 (2004) 5683.
[15] I. Fishtik, C.A. Callaghan, R. Datta, J. Phys. Chem. B 109 (2005) 2710.
[16] S. Kandoi, J. Greeley, M.A. Sanchez-Castillo, S.T. Evans, A.A. Gokhale, J.A. Dumesic, M. Mavrikakis, Top. Catal. 37 (2006) 17.
[17] A.A. Gokhale, S. Kandoi, J.P. Greeley, M. Mavrikakis, J.A. Dumesic, Chem. Eng. Sci. 59 (2004) 4679.
[18] P.C. Milner, J. Electrochem. Soc. 111 (1964) 228.
[19] J. Happel, P.H. Sellers, Adv. Catal. 32 (1983) 273.
[20] J.A. Dumesic, D.F. Rudd, L.M. Aparicio, J.E. Rekoske, A.A. Trevino, The Microkinetics of Heterogeneous Catalysis, Am. Chem. Soc., Washington, DC, 1993.
[21] E. Shustorovich, H. Sellers, Surf. Sci. Rep. 31 (1998) 1.
[22] H.S. Fogler, Elements of Chemical Reaction Engineering, fourth ed., Prentice Hall, Upper Saddle River, NJ, 2006.
[23] C.R.F. Lund, Ind. Eng. Chem. Res. 35 (1996) 2531.
[24] L.V. Gurvich, I.V. Veyts, C.B. Alcock, Thermodynamic Properties of Individual Substances, fourth ed., Hemisphere, New York, 1989.
[25] J.D. Cox, D.D. Wagman, V.A. Medvedev, CODATA Key Values for Thermodynamics, Hemisphere, New York, 1989.
[26] P.J. Linstrom, W.G. Mallard, National Institute of Standards and Technology, Gaithersburg, MD 20899, June 2005, http://webbook.nist.gov.
[27] M.J. Frisch, G.W. Trucks, H.B. Schlegel, G.E. Scuseria, M.A. Robb, J.R. Cheeseman, J.J.A. Montgomery, T. Vreven, K.N. Kudin, J.C. Burant, J.M. Millam, S.S. Iyengar, J. Tomasi, V. Barone, B. Mennucci, M. Cossi, G. Scalmani, N. Rega, G.A. Petersson, H. Nakatsuji, M. Hada, M. Ehara, K. Toyota, R. Fukuda, J. Hasegawa, M. Ishida, T. Nakajima, Y. Honda, O. Kitao, H. Nakai, M. Klene, X. Li, J.E. Knox, H.P. Hratchian, J.B. Cross, V. Bakken, C. Adamo, J. Jaramillo, R. Gomperts, R.E. Stratmann, O. Yazyev, A.J. Austin, R. Cammi, C. Pomelli, J.W. Ochterski, P.Y. Ayala, K. Morokuma, G.A. Voth, P. Salvador, J.J. Dannenberg, V.G. Zakrzewski, S. Dapprich, A.D. Daniels, M.C. Strain, O. Farkas, D.K. Malick, A.D. Rabuck, K. Raghavachari, J.B. Foresman, J.V. Ortiz, Q. Cui, A.G. Baboul, S. Clifford, J. Cioslowski, B.B. Stefanov, G. Liu, A. Liashenko, P. Piskorz, I. Komaromi, R.L. Martin, D.J. Fox, T. Keith, M.A. Al-Laham, C.Y. Peng, A. Nanayakkara, M. Challacombe, P.M.W. Gill, B. Johnson, W. Chen, M.W. Wong, C. Gonzalez, J.A. Pople, Gaussian 03, Rev. C. 02, Gaussian, Inc., Wallingford, CT, 2004.
[28] S.K. Desai, M. Neurock, K. Kourtakis, J. Phys. Chem. B 106 (2002) 2559.
[29] V.S. Bagotzky, Y.B. Vassiliev, O.A. Khazova, J. Electroanal. Chem. 81 (1977) 229.
[30] Multisim v. 9, Electronics Workbench, Prentice Hall Publishing.
[31] L.O. Chua, C.A. Desoer, E.S. Kuh, Linear and Nonlinear Circuits, McGraw–Hill, New York, 1987.
[32] J.W. Peck, D.I. Mahon, D.E. Beck, B. Bansenaur, B.E. Koel, Surf. Sci. 410 (1998).
[33] K. Franaszczuk, E. Herrero, P. Zelenay, A. Wieckowski, J. Wang, R.I. Masel, J. Phys. Chem. 96 (1992) 8509.